

Calculation model for layered glass

Ivica Kožar*¹ and Goran Šuran²

¹Faculty of Civil Engineering, University of Rijeka, Rijeka, Croatia

²KFK d.o.o., Dugo Selo-Rugvica, Croatia

(Received June 15, 2023, Revised August 31, 2023, Accepted September 4, 2023)

Abstract. This paper presents a mathematical model suitable for the calculation of laminated glass, i.e. glass plates combined with an interlayer material. The model is based on a beam differential equation for each glass plate and a separate differential equation for the slip in the interlayer. In addition to slip, the model takes into account prestressing force in the interlayer. It is possible to combine the two contributions arbitrarily, which is important because the glass sheet fabrication process changes the stiffness of the interlayer in ways that are not easily predictable and could introduce prestressing of varying magnitude. The model is suitable for reformulation into an inverse procedure for calculation of the relevant parameters. Model consisting of a system of differential-algebraic equations, proved too stiff for cases with the thin interlayer. This novel approach covers the full range of possible stiffnesses of layered glass sheets, i.e., from zero to infinite stiffness of the interlayer. The comparison of numerical and experimental results contributes to the validation of the model.

Keywords: differential equations; force-coupled structures; glazing; interlayer slip; laminated glass experiments; laminated glass model

1. Introduction

Glass is an extremely important building material for facade construction. Very often it is used for glazing in one-, two- or three-layer combinations. Typically (O'Regan 2015), glazing consists of glass sheets and a gas in between; sometimes it is ordinary air and sometimes argon or krypton gas. We distinguish between the thermal and structural properties of glass sheets. The properties of the gas between the glass sheets are important for the thermal (not the structural) behaviour of the glass. Regarding the structural behaviour, it can be treated as an ideal gas.

Moreover, what looks like a single pane of glass is often composed of two or more layers of glass with a special folium in between (laminated glass). This interlayer (folium) is between 0.38 and 6 mm thick and can be made of different materials: Polyester, acrylic, polyvinyl butyral (PVB), ethyl vinyl acetate (EVA), thermoplastic polyurethane (TPU), polyester (PET), etc. It is obvious that the properties of the interlayers are of great importance for the structural behaviour of the glass sheet as a whole.

In this paper, we present some challenges in modeling layered glass, in particular the influence

*Corresponding author, Professor, E-mail: ivica.kozar@gradri.uniri.hr

of the interlayer on the behavior of the glass plate, i.e., how does the processing of layered glass change the elastic modulus of a material that binds the glass plates together. At this stage, we neglect the viscous properties of the interlayer material, since the coupling with the glass is weak and can be accounted for later. Despite this simplification, this is an entry point to develop a model capable of fully describing the behavior of layered glass (similar to the approach for fiber reinforcement in Rukavina *et al.* 2019). This means that it is able to mimic the complete absence of a bond between the glass plates and also to model the complete bond that joins two materials into one.

The mechanism that binds the two plates consists of at least two parts: the sliding between the layers and the pre-stress between the layers. Because of the manufacturing process, which involves heating and thus develops a boundary layer between the interlayer and the glass plate, it is difficult to determine the exact contribution of each of these factors. The influence of the boundary layer is studied in (Challamel and Girhammar 2011), which assume uniformly distributed sliding forces or shear stresses between the layers. However, our model assumes a non-uniform distribution of strains and stresses. Besides analytical models, e.g., (Hartmann and Dileep 2019), semi-analytical models, e.g., (Gahleitner and Schoeftner 2021), there are also various numerical models, e.g., (Nikolić *et al.* 2018). Possible numerical finite element models include the use of flexural elements as in the MEPLA software (Bohmann 2015), solid 3D elements as in (Beton *et al.* 2023). It is possible to use extended elements combining properties of solid and flexural elements as in (Kožar *et al.* 2018).

Our first numerical model was based on a system of differential equations, one for each coupled beam, and was solved using a semi-analytical approach (see, e.g., Hirsh *et al.* 2004). The main advantage of this model is its multilayer nature, the accurate description of the force transfer between layers, and the accurate determination of the contribution of each layer to the structural stiffness. However, this model was too stiff for thin layers due to the large interlayer stiffness required for thin layers (a variety of models usually assume infinite transverse stiffness of the layers, e.g., Foraboschi 2009 or Campi and Monetto 2013), so we interrupted the development of this model for the time being.

Our novel mathematical model presented here is based on two beams with a common intermediate layer that generates only force coupling between the beams. By assuming infinite transverse stiffness of the intermediate layer, the equations are decoupled, similar to (Foraboschi 2009) and (Campi and Monetto 2013). Unlike the examples in the literature, this model includes both the sliding effect and the prestressing force in the interlayer and they can be freely mixed. It is important to consider variable parts of the influence of slip and prestress because the stiffness properties of the interlayer are highly variable and depend on many factors in the manufacture of the glass sheets. Once we learn more about the dependence of the structural properties of the interlayer on external influences, we will be able to determine the contribution of the two models in advance. More about material properties and their dependences on different parameters can be found in (Ibrahimbegovic 2009) or (Lemaitre and Chaboche 1994). Previous experience and formulation of a multilayer model are described in (Kožar *et al.* 2021), but this model is currently limited to two layers.

To validate the numerical model in terms of (Kožar *et al.* 2022), experiments were performed with a single plate and a two-layer plate. At this stage of the study, we did not perform a parametric analysis of the different thicknesses of the glass plates and the interlayer between them. Examples of more detailed experiments with two-layer glass plates can be found in (Araujo 2019).

The experiments performed are described in Section 2 of the paper, along with some statistical



Fig. 1 Experimental set-up with the detail of strain gauges for indirect displacement measurement

analyses that provide insight into the reliability of the results. The description of the numerical model follows in Section 3 with the formulation of the interlayer slip and the thermal bias resulting from the fabrication of the glass sheets. The comparison of the numerical results with the experimental results in Section 4 illustrates the properties of the model. Full validation of the mathematical model will be performed by parametric analysis with additional experimental tests in preparation.

2. Experimental analysis

The validation of the model is done by comparing it with the results of experiments carried out in two phases: i) bending tests on monolithic glass plates, and ii) bending tests on two-layer glass plates. The first group of experiments served to calibrate the measuring equipment. The second was used to validate the model for layered glass. We neglected the viscous properties of the interlayer. Our experiment is a three-point bending test with steel rollers as supports spaced 1.0 m apart and load applied via a steel roller in the centre of the plate (acting as a beam). The bending test is performed on two annealed glass plates with a size of 1.1 m×0.2 m and a thickness of 4.88 mm. The edges are ground smooth and covered with an intermediate layer of Trosifol Clear film of 0.76 mm initial thickness. The room temperature was 10°C and the loading time was about 10 minutes. The deformations were determined with a strain gauge. The load is applied via a steel roller, so there is no plate effect that would affect the beam model. The tests were performed in the KFK laboratory in Dugo Selo-Rugvica and the experimental setup is shown in Fig. 1.

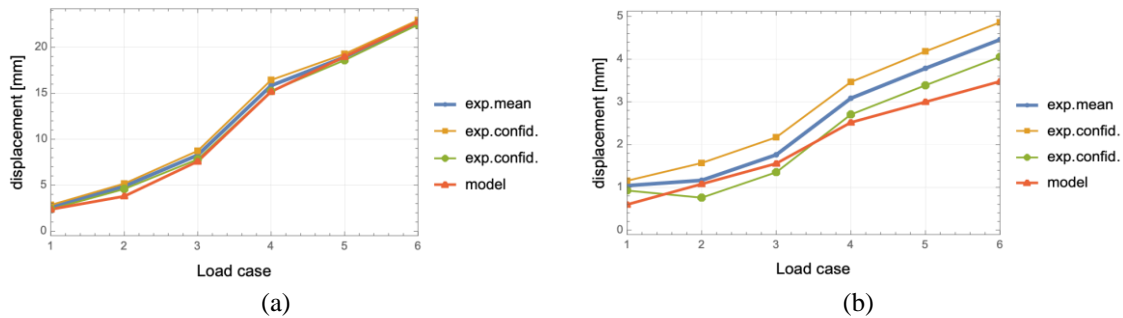


Fig. 2 Experimental measurements confidence interval and simple model: (a) monolithic glass displacements; (b) layered glass displacements

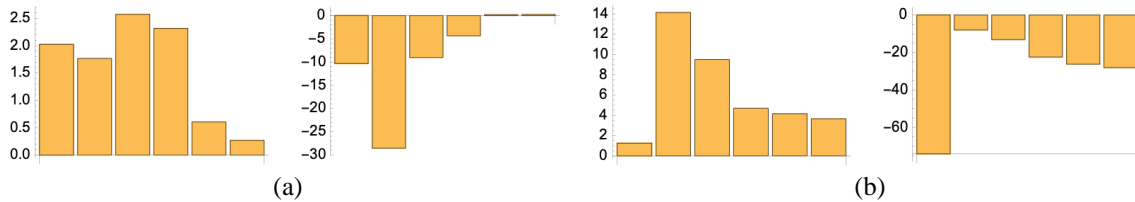


Fig. 3 Statistics of experimental measurements: (a) monolithic glass variance and difference from simple model; (b) layered glass variance and difference from simple model

In Fig. 1 we see the loading device, the supports and the device for measuring the displacement. The results of the experimental phases are shown in Figs. 2 and 3, i.e., the displacements due to self-weight and the displacements due to concentrated force loading. The loading is carried out until failure and the glass behaves as expected: brittle. We compare the displacements due to self-weight and gradually increasing loads, $P=\{0,25,0,50,1,00,1,25,1,50\}$ kN, where the behaviour of the glass remains linear. The experimental results are shown in Fig. 2 and the basic statistics in Fig. 3. In Fig. 2 we see the comparison of the experimental results with the simple model for the deflection of the centre of the beam, $\delta_q = \frac{5qL^4}{384EI}$ and $\delta_P = \frac{PL^3}{48EI}$. The definition of upper and lower deflection limits is for the orientation. In an example with a thicker interlayer, its thickness would be taken into account. The choice of moment of inertia I determines the limits of possible deflections. For the monolithic glass plate it is always the plate thickness, but for layered glass it can be the thickness of a single or double plate. The first gives the lower limit when the glass plates slide perfectly, and the second gives the upper limit when the bond between the plates is perfect. Note: The thickness of the layered glass is known (measured), but the thickness of the interlayer is not known. We assume that it is very thin, since the total thickness is 9.76 mm, which corresponds to two single glass plates (2×4.88 mm).

In Fig. 2(a) the model represents the displacement of a single plate and in Fig. 2(b) the model represents the lower bound, i.e., the displacement of two plates with perfect bond. Nevertheless, we see that the confidence line of the measurement is below the possible theoretical limit. The confidence interval in Fig. 2 is calculated with the equation $z \leq \left| \frac{\bar{x}-\mu}{\sigma} \right| \sqrt{N}$, where \bar{x} is the sample mean, μ is the unknown true mean, σ is the sample standard deviation, N is the number of samples and $z=1.96$ for the 95% confidence interval.

In Fig. 3 we see the simple statistics of the experimental measurements, Fig. 3(a) for the monolithic glass plate and Fig. 3(b) for the layered glass plate. The first bar graph shows the measurement reliability, i.e., the variation of the results for individual loads (from the smallest to the largest load). For both the monolithic plate and the layered glass plate, it is clear that the reliability increases with increasing load, i.e., a smaller force leads to less reliable measurement results. The second bar graph (with negative values) shows the discrepancy with the model predictions. For the monolithic plate, as the force increases, the results agree better and better with the model and are satisfactory for the self-weight. For the layered plate, the results deviate more from the model as the load increases and are particularly poor for the self-weight load (which is a rather small load). It could be said that the bond between the layers becomes weaker with increasing load, but the results for dead weight do not allow such a general conclusion. Definitely, the behaviour of interlayer bonding should be further investigated in a series of carefully planned experiments.

3. Mathematical model

Our mathematical model is presented using an example of two beams coupled with an intermediate layer. In addition to the coupling due to the interlayer, there is also a prestress coupling due to thermal effects that occur during the manufacture of the laminated glass plate. Each of the models alone is capable of mimicking both displacement limits, the lower one for the case where there is no coupling and the upper one for the case where the interlayer is perfectly coupled. In order to use realistic material parameters, we must use both models simultaneously. At this stage of the study, the plates are simply supported and treated mathematically as beams. This simplifies the study of the behaviour of the intermediate layers. We have also assumed small displacements and strains.

3.1 Air coupled glass model

For the sake of completeness, we will mention only the air-coupled glass model. If we have two glass plates with a gas (e.g., air) between them, the displacements of the plates are coupled to the gas pressure acting on both. The ideal gas equation acting on the volume (between the beams/plates) is the coupling equation. The normalised system of equations is

$$\begin{aligned} \frac{d^4 y_1(x)}{dx^4} + (y_1(x) - y_2(x))P_t &= p(x) \\ \frac{d^4 y_2(x)}{dx^4} - (y_1(x) - y_2(x))P_t &= 0 \end{aligned} \quad (1)$$

$$P_0 V_0 T = P_t V_t T \quad , \quad V_t = V_0 - \int y_1 + \int y_2$$

The above equation represents two glass plates treated as beams coupled with the ideal gas equation, where y_i is the beam displacement, P_t is the gas pressure after loading, P_0 is the initial gas pressure, V_0 and V_t represent the gas volume before and after the loading.

We have not yet studied this type of glass experimentally and a study is planned for future development.

3.2 Model of interlayer slip

In the layered glass model, the glass plates are strongly coupled and their behaviour could not be modelled by pressure transfer (at high pressure values, the system of equations becomes stiff). The basic assumptions of layered coupling (see, e.g., Foraboschi 2009) are that each layer is elastic and the Bernoulli-Navier hypothesis is satisfied and that the vertical layer displacements are the same for each layer (and consequently the curvatures are the same), there is only the shear stress in the interlayer (except for the axial stress from the eventual prestress, i.e., from the axial thermal stress). This assumption is equivalent to the hypothesis that the longitudinal modulus of elasticity is zero and the transverse modulus of elasticity is infinite.

Our model assumes that laminated glass dissipates most of its deformation energy by bending the layers, with an intermediate layer serving as a means of redistributing the load among the layers. In the interlayer, we assume the existence of an elastic stress tensor $\begin{bmatrix} 0 & \tau \\ \tau & \sigma \end{bmatrix}$, where zero stress refers to stress perpendicular to the glass plates, σ is parallel to the glass plates, and τ is shear. The components of the stress tensor are additively decomposed into the shear, which is always present, and the axial stress, which we believe is also always present, but without a definite cause (at the moment). To explain, let us assume that the upper beam deforms by a certain value $f(x)$. In this simple model, the lower beam is offset from the upper beam by a distance h , so its deformation is $f(x)+h$. The lengths of these two beams are not equal. The length of the first beam is $\int_0^x f(\tau)d\tau$ and that of the second $\int_0^x f(\tau)d\tau + \frac{hx}{2}$, so that an axial force acts in the intermediate layer even without any prestressing. Note that the shear stress contribution τ “hides” an influence of the interlayer thickness h since $\tau = \gamma G_S = \frac{\xi}{h} G_S$.

To simplify the problem, we could write the beam equation as a function of the bending moment $EIy''(x) = M(x)$ and treat coupled beam equations as separate equations, each with its own bending moment. Thus, we have $M_A(x)$ acting on the upper beam and $M_B(x)$ acting on the bottom beam, see Fig.4.b). The assumption that the beams have equal displacements leads to equal bending moments, $M_A(x)=M_B(x)$. This assumption is adopted by many researchers and is discussed elsewhere in this paper.

The interlayer forces resulting from the slipping of the beam act as additional forces in the cross section. They can be compared to the prestressing force acting in the interlayer, but in the opposite direction for each beam producing opposite prestressing moments. The mechanics of the development of the interlayer stresses are shown in Fig. 4(a) and the resulting prestressing force N_T in Fig. 4(b). Fig. 4(b) also shows possible stress distributions in the beam cross sections.

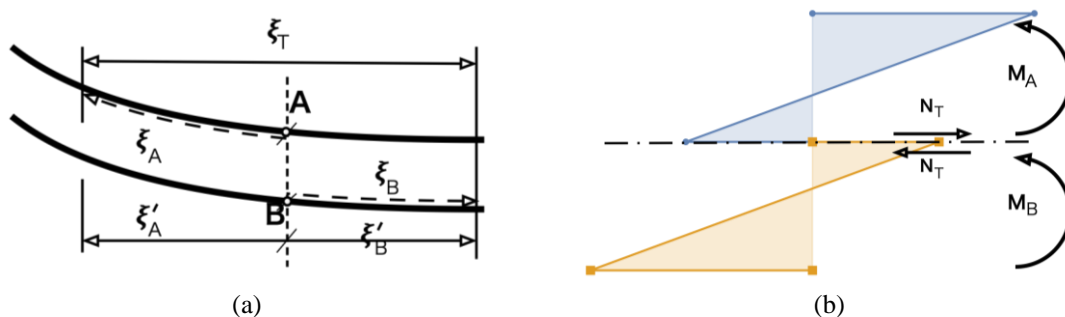


Fig. 4 (a) Slipping of the upper and lower beams; (b) external moments acting on the cross sections of the upper and lower beam

The mathematical formulation of the problem is as follows

$$\begin{aligned}
 M_A(x) &= p_0(M_P(x) + M_q(x) + M_T(x)) \\
 M_B(x) &= (1 - p_0)M_A(x) \\
 M_T(x) &= \frac{b_0 h_A}{2} E_S \int_0^x \xi(\tau) d\tau \\
 \sigma_A^d(x) &= \frac{M_A}{W_A}, \quad \sigma_B^u(x) = \frac{M_B}{W_B} \\
 \xi_T(x) &= \xi_B(x) - \xi_A(x) \quad (2) \\
 \frac{d\xi(x)}{dx} &= \epsilon(x) = \frac{\sigma(x)}{E} \\
 S(x) &= \frac{1}{E_A} \frac{d\sigma_A^d(x)}{dx} + \frac{1}{E_B} \frac{d\sigma_B^u(x)}{dx} \\
 \frac{d^2 \xi_T(x)}{dx^2} + S(x) &= 0, \quad \xi_T'(0) = 0, \quad \xi_T\left(\frac{L}{2}\right) = 0
 \end{aligned}$$

In the above system of Eq. (2), equations are substituted one into another so only the last differential equation remains to be solved. The meaning of the symbols is as follows:

M_p, M_q, M_T -respectively, external moment from forces, self-weight and prestress

ξ, ϵ -respectively, the slip function and the strains

A, B, d, u -respectively, indices for upper and lower beam, for down and upper side of the beams

σ, W, E -respectively, stresses and the section moduli, material moduli.

As a consequence of assuming equal beam deflections, p_0 is assumed to be 1/2. Using p_0 instead of the constant enables us to enhance the formulation with different assumptions that would not result in equal beam deflections. However, that is left for future development.

The system of Eq. (2) is combined with beam differential equation

$$E_1 I_1 \frac{d^2 y_1}{dx^2} + M_A(x) = 0 \quad (3)$$

where index ‘1’ stands for the upper beam and index ‘2’ for the lower one. This equation is later used for displacement calculation.

The system of Eq. (2) is quite large, and although we could substitute individual equations into the final differential equation, we have not done so. Instead, WolframMathematica performs the substitutions and solves the final system. The advantage is that the intermediate results are available for review and one gets a better insight into the solution procedure. Also, solving in closed form imposes restrictions on the system that can be solved and makes further extensions more difficult.

3.3 Prestressing

In the manufacture of laminated glass, the glass and the interlayer (e.g., polyvinyl butyral) are heated and cooled. The elastic moduli and coefficients of thermal expansion of the two materials in laminated glass are different, resulting in the development of thermal strains and stresses. The evolution of thermal residual stress in a combination of elastic (glass) and viscoelastic materials (PVB) is interesting and non-trivial. However, here we will apply the simplest reasonable coupling of layers to estimate the residual axial force that affects the deflection of the beam.

We assume that the two materials are tightly coupled and have equal longitudinal displacements, i.e., strains, since their lengths are equal. The equation for the strains is

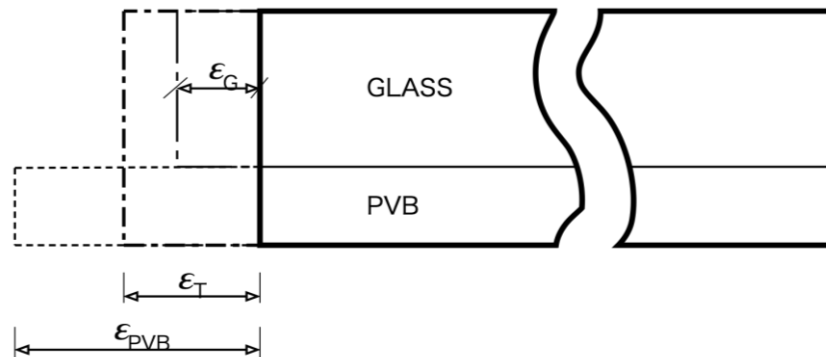


Fig. 5 Assumed thermal prestress behaviour

$$\frac{\sigma_1}{E_1} + \alpha_1 \Delta T = \frac{\sigma_2}{E_2} + \alpha_2 \Delta T \quad (4)$$

In the above equation ΔT is the temperature difference, σ_i is the stress, E_i is the modulus and α_i is the coefficient of thermal expansion of the layer i . The introduction of the force equation $\sigma_1 A_1 = \sigma_2 A_2$ allows us to find suitable stresses and the corresponding axial force, i.e., the thermal prestress. Note: We assume that the heating occurs on a flat surface and that there is no contribution from bending. The introduction of bending during heating would extend the possible variations of the pre-stress of the layered glass.

Thermal prestressing is only one example of a possible additional axial force. It is not the only possible source of the axial force, i.e., the shrinkage of the interlayer can have various causes, not only the thermal change. At this stage, the forces in the interlayer are not our research subject and we have not attempted to study the processes in the interlayer because this requires lengthy experiments with sophisticated equipment; this is planned for our future research.

4. Numerical example

The examples were calculated using differential equations with Wolfram Mathematica. It is possible to use numerical methods, but for the proof of concept it was faster to use the methods provided by Wolfram. The beams have equal geometrical and material properties, width=0.2 m, length=1.0 m, two glass layers with height=4.88 mm each and negligible height of the intermediate layer (the exact value after joining the two glass plates could not be determined). The modulus of elasticity for glass is 70 GPa, for the interlayer: $E_S=3$ MPa (assumed because it might have changed after heating). The load $P(x)$ is the point load at the centre of the upper beam with values $P=\{0,0.025,0.05,0.1,0.125,0.15\}$ kN in combination with the self-weight.

For better illustration and comparison of the results, we have calculated the upper and lower limits of the displacement of the layered glass beam. The lower limit is the deflection of two uncoupled glass plates (at self-weight equal to the deflection of a single glass plate, since the plates slide freely over each other) and the upper limit is the deflection of two perfectly coupled (confined) glass plates (equal to the deflection of a single glass plate of double thickness, since the plates are coupled so that there is no sliding between them). All of our results should fall between these two limits.

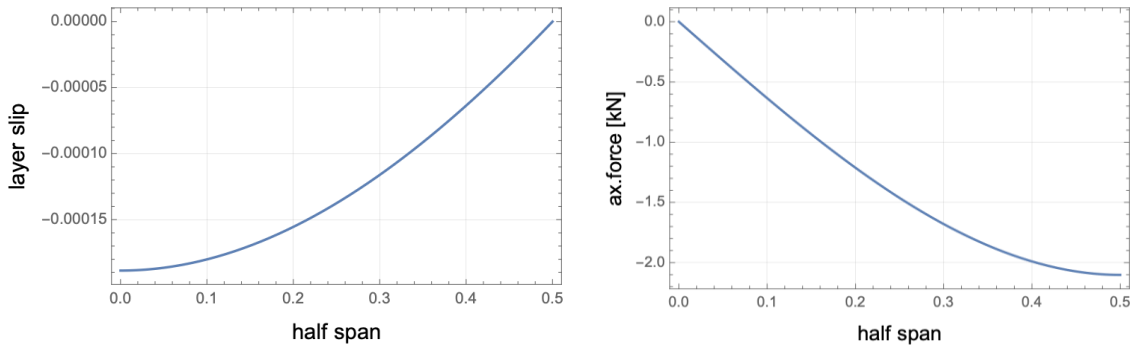


Fig. 6 Along the half span of the beam, a) interlayer slip and b) the resulting axial force

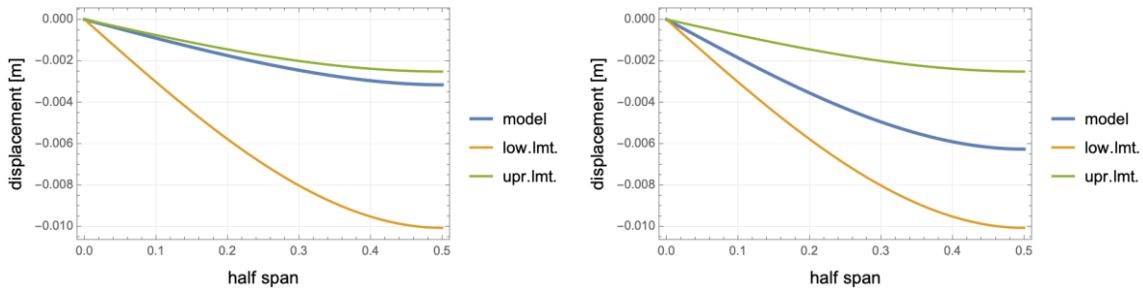


Fig. 7 Comparison of layered glass displacement with interlayer slip and with a) and without b) the additional axial force

4.1 Interlayer coupling

The contribution of interlayer coupling is described by Eq. (2) and the resulting total slip function ξ_T is presented in Fig. 6(a). It can be seen that the slip is maximum at the edge of the beam and zero at the centre. The axial force in the intermediate layer is nonlinear and is shown in Fig. 6(b). It is a summation of the contributions along the beam, $N_T(x) = E_S \int_0^x \xi(\tau) d\tau$, with extremes opposite to the slip function: Zero at the edge and maximum at the centre of the bar.

The exact values in Fig. 6 change with the material parameters and the load. The values shown here correspond to the load $P=0.1$ kN.

The axial force is calculated from strain as $N_T = E_S \int_0^x \xi(\tau) d\tau$, so that its value is zero at the end. This is consistent with the fact that the internal forces cannot exert an external force on free parts of the structure.

4.2 Axial stress

The production of the layered glass in this example involved heating to 60 degrees Celsius (on a flat surface), after which the two glass plates were firmly bonded together. The exact material parameters after heating are not known, so we assume data from literature/the Internet: $\alpha_{glass}=5.9E-6$, $\alpha_{PVB}=139E-6$, $E_{glass}=70$ GPa, $E_{PVB}=3$ MPa and $\Delta T=-40^\circ C$. With these data, Eq. (4) gives $N_T=2.444$ kN. This axial force is constant along the beam and visibly reduces the displacement of the layered glass for all loading cases.

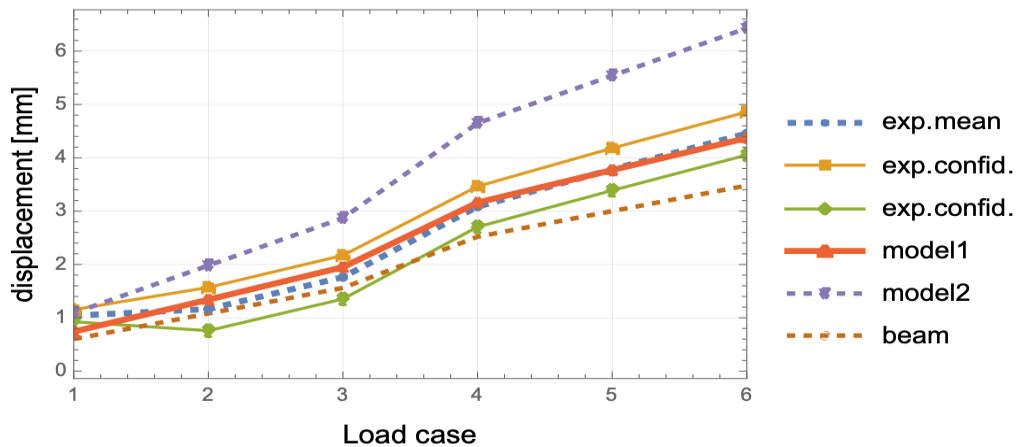


Fig. 8 Comparison of the experimental results and model calculation with various parameters

The comparison of the displacements with respect to the lower and upper limits is shown in Fig. 7. It is obvious that either the intermediate layer with sufficient stiffness or the axial force sufficiently large can reproduce any value within the indicated limits. However, the internal forces corresponding to the cases in Fig. 7 are not identical, as will be explained (see Fig. 9).

The displacements in Fig. 7 are generated using Eq. (3) and Eq. (2). It is interesting to note that the relationship of the displacements (with respect to the limits) is approximately preserved for the chosen E_S and N_T with respect to the load; this remains to be investigated.

4.3 Resulting displacements and stresses

The validation of our mathematical model is done by comparing the calculated displacements with the experimental results. In Fig. 8 we show this comparison for different model parameters together with the confidence limits for the experimental results. The term “beam” represents the displacements of the monolithic glass plate and is the minimum displacement theoretically possible. The term “Model1” stands for our model with $E_S=3$ MPa and $N_T=3$ kN, which shows excellent agreement with the experimental results. The term “Model2” stands for our model with $E_S=70$ GPa and $N_T=0$ kN, whose results are too large. However, with a further increase of E_S , which is not physically justified, it is possible to obtain a very good agreement as well.

In both models, the axial force is always present due to slip, while “Model 1” has an additional preloaded axial force N_T . At the moment, the values of E_S and N_T are assumed, but since this model is suitable for formulating the inverse problem (that is the only purpose of this model), they will be determined from the experiments in the future.

The displacements are the only measured quantities we could compare, but it is instructive to show some other results as well. In Fig. 9 we present internal parameters: the stress distribution in the centre of the upper and lower glass plates. Fig. 9(a) shows the distribution for the “Model1” from Fig. 8 and Fig. 9(b) for the “Model2”.

It is interesting to note that the shape of stresses remains approximately the same as we increase the parameter value in the model. In other words, with physically unjustified parameters, even with “Model2”, which has the stress distribution from Fig. 9(b), we could obtain excellent results of “Model1” that has the stress distribution from Fig. 9(a). The two models are mixed in reality but

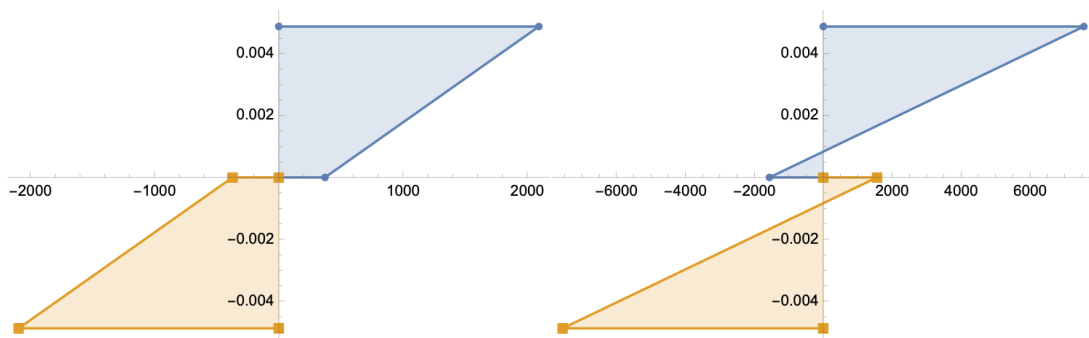


Fig. 9 Comparison of the stress profile for the model displacement equal to the experimental: (a) large interlayer modulus and axial force $N_p=0$ kN, (b) small interlayer modulus and axial force $N_p=3$ kN

the “correct” ratio of the mixture could be known only from experiments. Therefore, we plan additional experiments in which the stress distribution is evaluated in some way, perhaps by observing the displacement of the plate edges, if nothing else. Subsequently, the mixing ratio could be determined as a parameter of the model, similar to (Kožar *et al.* 2018).

5. Conclusions

In our analysis, we have identified two key parameters, the interlayer stress and the axial preload force, which determine the displacement of the layered glass sheet. Their influence is most easily explained by the change in moments acting on the beam. In this approach, the analysis of layered glass is divided among the contributions of each layer in conjunction with the interlayer that connects them. This approach simplifies the mathematical model and an eventual formulation of the optimization procedure for parameter estimation, which is planned as a future development. We also plan to use plate equations instead of beam equations for modelling glass layers in future work.

However, determining the exact behaviour of the interlayer, its real elastic modulus when compressed in a thin layer between two glass plates, and its behaviour during heating would require additional, more detailed and accurate measurements.

Acknowledgments

This work was supported by project HRZZ 7926 “Separation of parameter influence in engineering modeling and parameter identification”, project KK.01.1.1.04.0056 “Structure integrity in energy and transportation” and University of Rijeka grant ‘uniri-tehnic-18-108’, for which we gratefully acknowledge.

References

Araujo, T.J.P. (2019), “Experimental and numerical analysis of two-layer composite beams”, Thesis,

- Instituto Superior De Engenharia De Lisboa
- Bedon, C., Markovic, D., Karlos, V. and Larcher, M. (2023), "Numerical investigation of glass windows under near-field blast", *Couple. Syst. Mech.*, **12**, 167-181. <https://doi.org/10.12989/csm.2023.12.2.167>.
- Bohmann, D. (2015), *SJ MEPLA Theory Manual*, SJ Software GmbH, Aachen.
- Campi, F. and Monetto, I. (2013), "Analytical solutions of two-layer beams with interlayer slip and bi-linear interface law", *Int. J. Solid. Struct.*, **50**, 687-698. <http://doi.org/10.1016/j.ijsolstr.2012.10.032>.
- Challamel, N. and Girhammar, U.A. (2011), "Boundary layer effect in composite beams with interlayer slip", *J. Aerosp. Eng.*, ASCE, **24**(2), 199-209. [https://doi.org/10.1061/\(ASCE\)AS.1943-5525.0000027](https://doi.org/10.1061/(ASCE)AS.1943-5525.0000027).
- Foraboschi, P. (2009), "Analytical solution of two-layer beam taking into account nonlinear interlayer slip", *J. Eng. Mech.*, **135**(10), 1129-1146. [https://doi.org/10.1061/\(ASCE\)EM.1943-7889.0000043](https://doi.org/10.1061/(ASCE)EM.1943-7889.0000043).
- Gahleitner, J. and Schoeftner, J. (2021), "A two-layer beam model with interlayer slip based on two-dimensional elasticity", *Compos. Struct.*, **274**, 114283. <https://doi.org/10.1016/j.compstruct.2021.114283>.
- Hartmann, S. and Dileep, P.K. (2019), "Classical beam theory with arbitrary number of layers", Technical Report Series, Technische Universität Clausthal.
- Hirsh, M.W., Smale, S. and Devaney, R.L. (2004), *Differential Equations, Dynamical Systems and An Introduction to Chaos*, Elsevier, Amsterdam.
- Ibrahimbegovic, A. (2009), *Nonlinear Solid Mechanics: Theoretical Formulations and Finite Element Solution Methods*, Vol. 160, Springer, Science & Business Media.
- Ibrahimbegovic, A. and Markovic, D. (2003), "Strong coupling methods in multi-phase and multi-scale modeling of inelastic behavior of heterogeneous structures", *Comput. Meth. Appl. Mech. Eng.*, **192**, 3089-3107. [https://doi.org/10.1016/S0045-7825\(03\)00342-6](https://doi.org/10.1016/S0045-7825(03)00342-6).
- Kožar, I. and Ožbolt, J. (2010), "Some aspects of load-rate sensitivity in visco-elastic microplane model", *Comput. Concrete*, **7**, 317-329. <https://doi.org/10.12989/cac.2010.7.4.317>.
- Kožar, I., Bede, N., Mrakovčić, S. and Božić, Ž. (2021), "Layered model of crack growth in concrete beams in bending", *Procedia Struct. Integrity*, **31**, 134-139. <https://doi.org/10.1016/j.prostr.2021.03.022>.
- Kožar, I., Bede, N., Mrakovčić, S. and Božić, Ž. (2022), "Verification of a fracture model for fiber reinforced concrete beams in bending", *Eng. Fail. Anal.*, **138**, 106378. <https://doi.org/10.1016/j.engfailanal.2022.106378>.
- Kožar, I., Rukavina, T. and Ibrahimbegovic, A. (2018), "Method of incompatible models-Overview and applications", *Gradevinar*, **70**, 19-29. <https://doi.org/10.14256/JCE.2078.2017>.
- Kožar, I., Torić Malić, N. and Rukavina, T. (2018), "Inverse model for pullout determination of steel fibers", *Couple. Syst. Mech.*, **7**, 197-209. <https://doi.org/10.12989/csm.2018.7.2.197>.
- Lemaitre, J. and Chaboche, L.J. (1994), *Mechanics of Solid Materials*, Cambridge University Press, Cambridge.
- Nikolić, M., Karavelić, E., Ibrahimbegovic, A. and Mišćević, P. (2018), "Lattice element models and their peculiarities", *Arch. Comput. Meth. Eng.*, **25**(3), 753-784. <https://doi.org/10.1007/s11831-017-9210-y>.
- O'Regan, C. (2015), *Structural Use of Glass in Buildings*, The Institution of Structural Engineers, London.
- Rukavina, T., Ibrahimbegovic, A. and Kožar, I. (2019), "Fiber-reinforced brittle material fracture models capable of capturing a complete set of failure modes including fiber pull-out", *Comput. Meth. Appl. Mech. Eng.*, **192**, 3089-3107. <https://doi.org/10.1016/j.cma.2019.05.054>.
- Wolfram Research Inc., Mathematica (2023), <https://www.wolfram.com/mathematica/>